

De Broglie Waves – John Macken

The following excerpts from my book deal with de Broglie waves.

The following is from pages 1-5 to 1-10 in my book. Later other pages are quoted.

de Broglie Waves: The similarity between confined light and particles does not end with the confined light possessing rest mass, weight and kinetic energy when there is relative motion. Next we will examine the similarity between the wave characteristics of confined light and the de Broglie wave patterns of fundamental particles. For example, particles with mass m and velocity v that pass through a double slit produce an interference pattern which can be interpreted as having a de Broglie wavelength λ_d given by the equation:

$$\lambda_d = h/p \quad \text{where } \lambda_d = \text{de Broglie wavelength; } h = \text{Planck's constant; } p = \text{momentum}$$

$$\lambda_d = h/\gamma m_o v \quad \text{where } \gamma = \frac{1}{\sqrt{1-v^2/c^2}} \quad m_o = \text{particle's rest mass}$$

$$\nu_d = E/h \quad \text{where } \nu_d = \text{de Broglie frequency } E = \text{total energy}$$

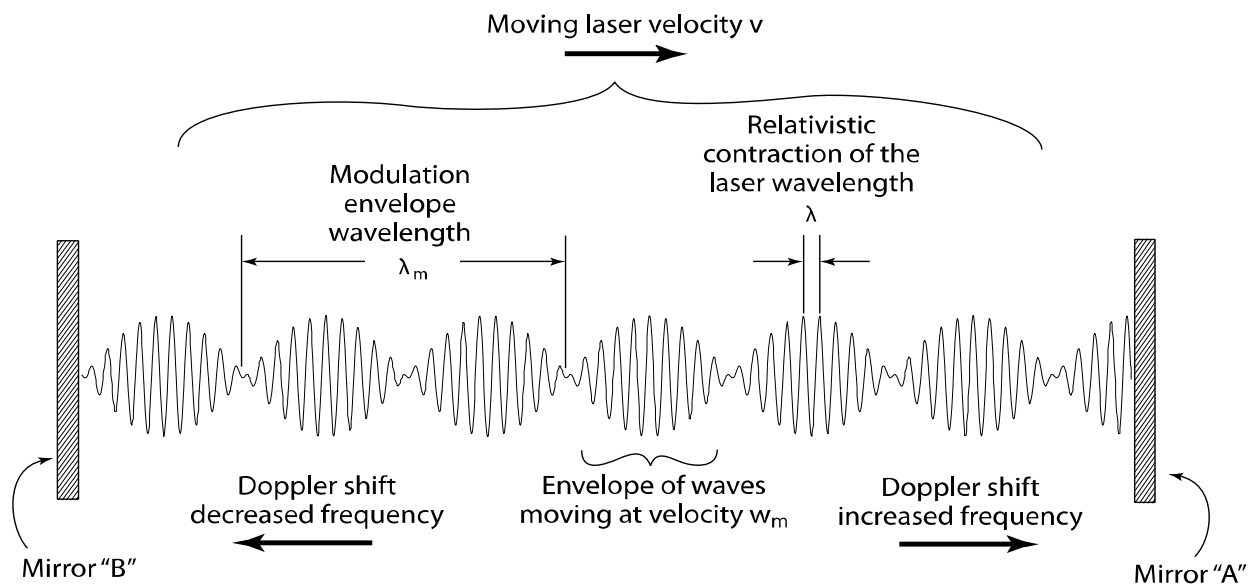


FIGURE 1-1 Wave pattern present in a moving laser due to Doppler shifts on the bi-directional light waves

The de Broglie waves have a phase velocity $w_d = c^2/v$ and a group velocity $u_d = v$. The phase velocity w_d is faster than the speed of light and the group velocity, u_d , equals the velocity of the particle, v .

There is a striking similarity between the de Broglie wave characteristics of a moving particle and the wave characteristics of confined light in a moving laser. Figure 1-1 shows a moving laser with mirrors A and B reflecting the light waves of a laser beam. Figure 1-1 is a composite because the light wave depicts electric field strength in the Y axis while the mirrors are shown in cross section. If the laser is stationary, the standing waves between the mirrors would have maximum electric field amplitude that is uniform at any instant. However, the laser in Figure 1-1 is moving in the direction of the arrow shown at velocity v . From the perspective of a “stationary” observer, light waves propagating in the direction of velocity v are Doppler shifted up in frequency, and light waves moving in the opposite direction are shifted down in frequency. When these electric field amplitudes are added, this produces the modulation envelope on the Doppler shifted bidirectional light in the laser as perceived by a stationary observer. This modulation envelope propagates in the direction of the translation direction but the modulation envelope has a velocity (w_m) which is faster than the speed of light ($w_m = c^2/v$) (calculated in appendix A). This is just an interference pattern and it can propagate faster than the speed of light without violating the special relativity prohibition against superluminal travel. No message can be sent faster than the speed of light on this interference pattern. The modulation envelope has a wavelength λ_m where:

$$\lambda_m = \frac{\lambda_\gamma c}{v} \quad \lambda_m = \text{modulation envelope wavelength}; \lambda_\gamma = \text{wavelength of confined light}$$

As seen in figure 1-1, one complete modulation envelope wavelength encompasses two nulls or two lobes. It will be shown later that there is a 180 degree phase shift at each null, so to return to the original phase requires two reversals (two lobes per wavelength).

The similarity to de Broglie waves can be seen if we equate the energy of a single photon of wavelength λ_γ to the energy of a particle of equivalent mass m . This will assume the non-relativistic approximation. Appendix A will address the more general relativistic case.

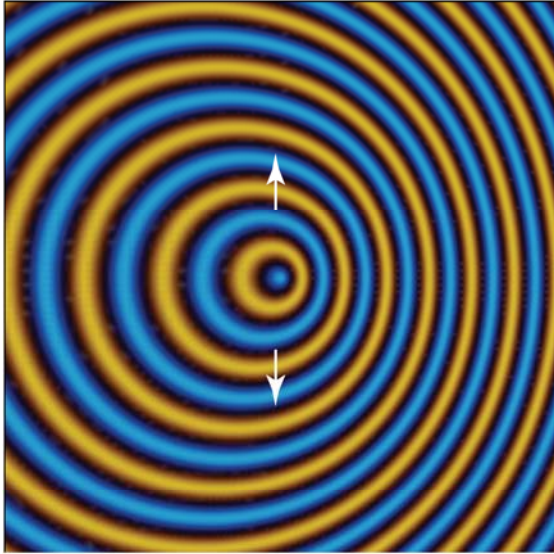
$$E = \frac{hc}{\lambda_\gamma} = mc^2 \quad \text{equating photon energy to mass energy therefore } m = \frac{h}{c\lambda_\gamma}$$

$$\lambda_d = \frac{h}{mv} \quad \lambda_d = \text{de Broglie wavelength;}$$

$$\lambda_d = \frac{\lambda_\gamma c}{v} = \lambda_m \quad \text{de Broglie wavelength } \lambda_d = \text{modulation envelope wavelength } \lambda_m$$

The modulation envelope not only has the correct wavelength, it also has the correct phase velocity ($w_d = w_m = c^2/v$). The “standing” optical waves also have a group velocity of v . Therefore these waves move with the velocity of the mirrors and appear to be standing relative to the mirrors.

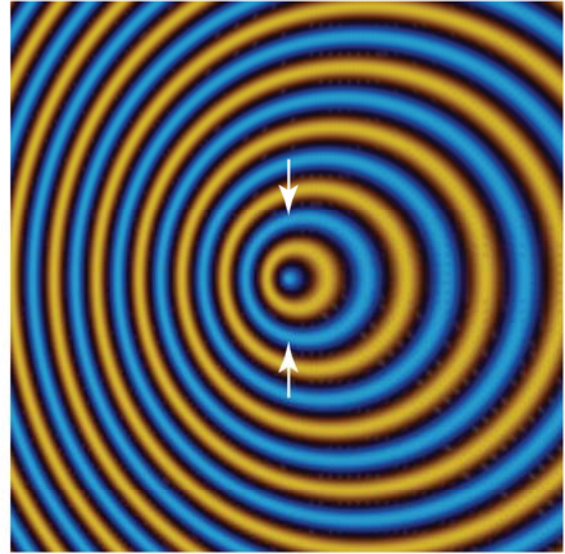
Outward propagating waves



Direction of motion

FIGURE 1-2 Doppler shift on outward propagating waves

Inward propagating waves



Direction of motion

FIGURE 1-3 Doppler shift on inward propagating waves

de Broglie Waves in Radial Propagation: It is easy to see how the optical equivalent of de Broglie waves can form in the example above with propagation along the axis of translation. However, it is not as obvious what would happen if we translated the laser in a direction not aligned with the laser axis. We will take this to the limit and examine what happens when the waves propagate radially into a 360° plane that is parallel to the translation direction. To understand what happens, we will first look at figure 1-2 that shows the Doppler shifted wave pattern produced by waves propagating away from a point source in a moving frame of reference. The source is moving from left to right as indicated by the arrow. Waves moving in the direction of relative motion (to the right) are seen as shifted to a shorter wavelength and waves moving opposite to the direction of travel are shifted to a longer wavelength. Figure 1-3 is similar to figure 1-2 except that only waves propagating towards the source are shown.

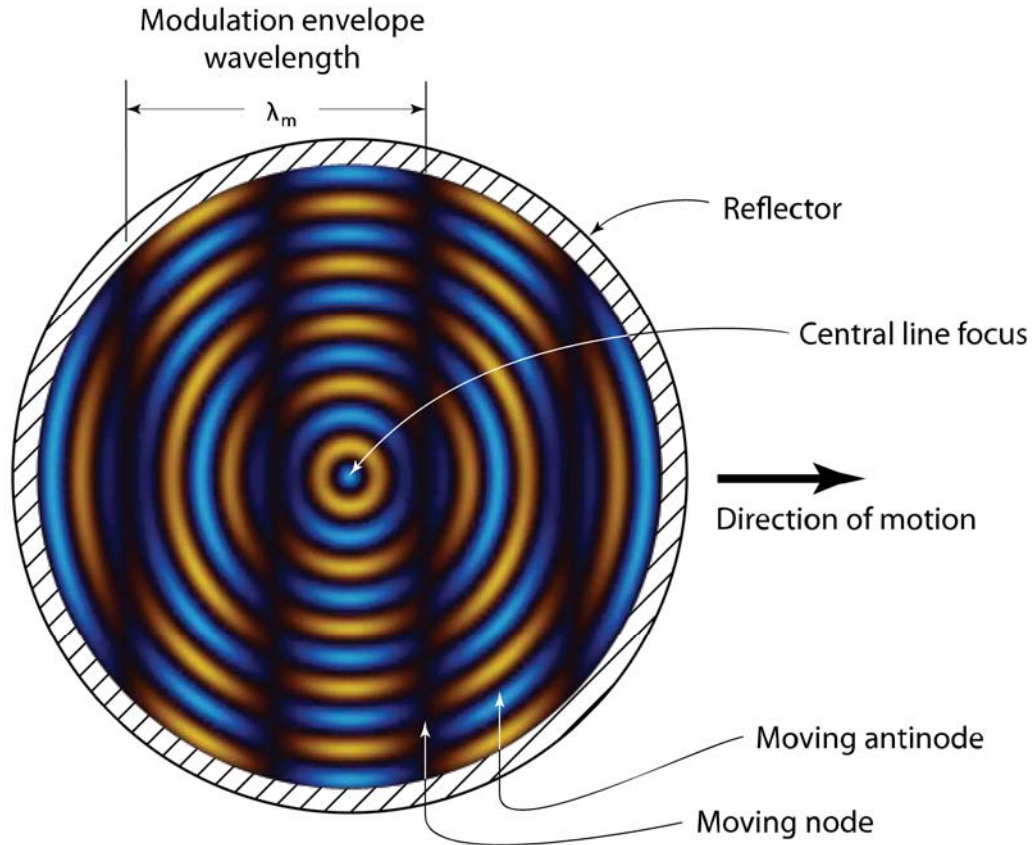


FIGURE 1-4 Wave pattern produced when radially propagating standing waves are observed in a moving frame of reference

Figure 1-4 shows what happens when we add together the outward and inward propagating waves shown in figures 1-2 and 1-3. Also a cross-sectioned cylindrical reflector has been added to figure 1-4. This reflector can be thought of as the reason that there are waves propagating towards the center. The central lobe of figure 1-4 can be thought of as a line focus that runs down the axis of the cylindrical reflector.

The vertical dark bands in figure 1-4 correspond to the null regions in the modulation envelope. These null regions can be seen in figure 1-1 as the periodic regions of minimum amplitude. There is a 180° phase shift at the nulls. This can be seen by following a particular fringe through the dark null region. If the wave is represented by a yellow color on one side of the null, this same wave is a blue color on the other side of the null. This color change indicates that a 180° phase shift occurs at the null. In figure 1-1, the reason that the wavelength of the modulation envelope λ_m is defined as including two lobes is because of this phase reversal that happens at every null. Therefore it takes two lobes to return to the original phase and form one complete wavelength.

The main purpose of this figure is to illustrate that de Broglie waves with a plane wavefront appear even in light that is propagating radially. This is a modulation envelope that is the

equivalent of a plane wave moving in the same direction as the relative motion, but moving at a speed faster than the speed of light. Figure 1-4 represents an instant in a rapidly changing wave pattern.

There has also been an artistic license taken in this figure to help illustrate the point. Normally we would expect the electric field strength to be very large along the focal line at the center of the cylindrical reflector and decrease radially. However, accurately showing this radial amplitude variation would hide the wave pattern that is the purpose of this figure. Therefore the radial amplitude dependence has been eliminated to permit the other wave patterns to be shown. Another artistic license is the elimination of the Guoy effect at the line focus. The central lobe of a cylindrical focus should be enlarged by $\frac{1}{4}$ wavelength to accommodate the 90° phase shift produced when electromagnetic radiation passes through a line focus. Ultimately we will be transferring the concepts illustrated here to a different model that does not require this slight enlargement.

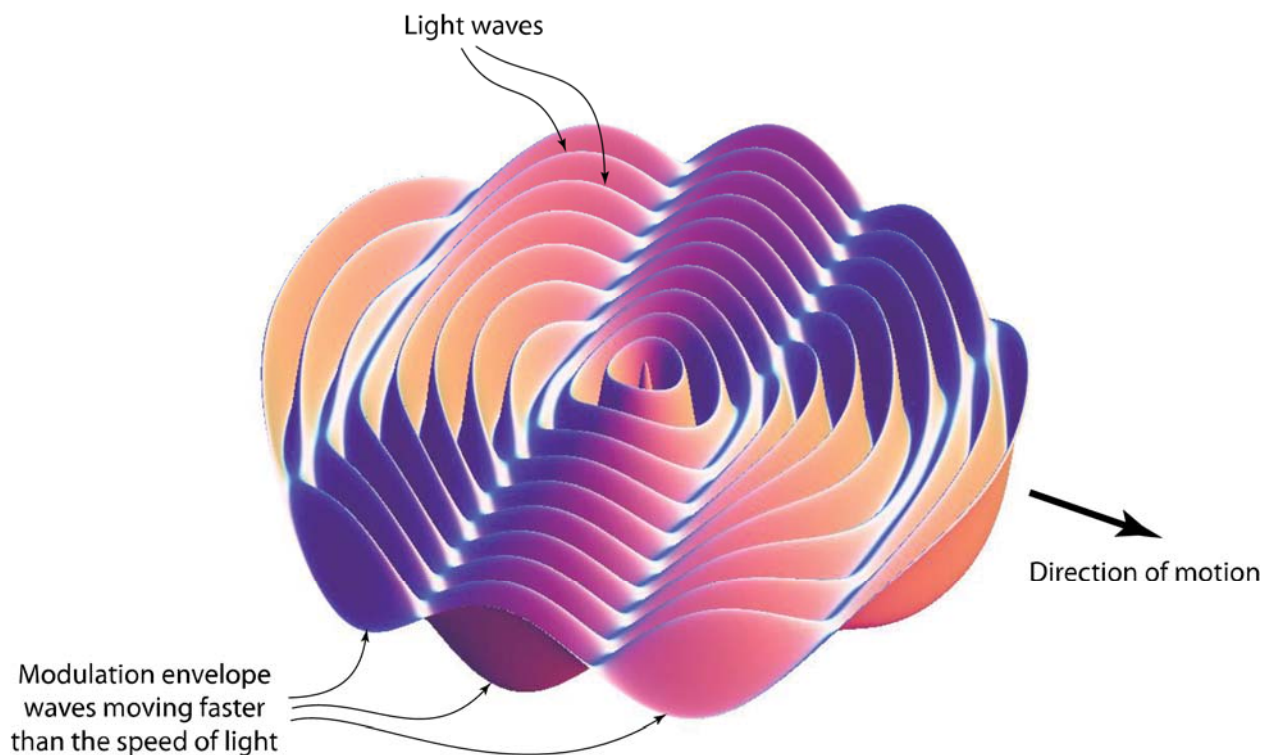


FIGURE 1-5 A three-dimensional representation of figure 1-4 where the Z axis is used to represent electric field

Figure 1-5 is a 3 dimensional representation of the wave pattern present in figure 1-4. In figure 1-5 the Z axis is used to represent the electric field. The cylindrical reflector has been removed from the illustration to permit the waves to be seen. Also as before, the radial amplitude dependence has been eliminated to permit the subtle modulation envelope to be seen. If figure 1-5 was set in motion, the concentric circular wave pattern would move as a unit. However,

superimposed on this is the moving envelope of waves that are moving through this wave structure (waves on waves). This moving envelope of waves is moving faster than the speed of light in the same direction as overall motion ($w_m = c^2/v$).

The surprising part of figure 1-4 and 1-5 is that we obtain a linear modulation envelope imposed on the radial propagating waves. It does not make any difference what the propagation angle is, the equivalent of de Broglie waves are produced for all angles. The only requirement is that the wave has bidirectional propagation. If later we are successful in establishing a model of fundamental particles that exhibits bidirectional wave motion, that model will also exhibit de Broglie waves.

Next we are going to talk about relativistic length contraction. For illustration, we will return to figure 1-1. This figure shows the wave frozen in time and designates the distance that approximately corresponds to the laser wavelength λ . Actually, this distance only precisely equals the laser wavelength when there is no relative motion. In the example illustrated in figure 1-1, there is relative motion. The wave illustrated is the result of adding together a wave that has been Doppler shifted up in frequency to a wave that has been Doppler shifted down in frequency. The combination produces a peak to peak distance that is equal to the relativistic contraction of the laser wavelength.

This is reasonable when you consider that there are a fixed number of standing waves between the two mirrors. If the distance between the two mirrors undergoes a relativistic contraction, the standing waves must also exhibit the same contraction to retain the fixed number of standing waves. However, it is possible to reverse this reasoning. Rather than saying that the standing waves must contract to fit between the relativistic contracted mirror separation, it is possible to say that we might be getting a fundamental insight into the mechanics of how nature accomplishes relativistic contraction of physical objects. If all fundamental particles and forces of nature can ultimately be reduced to bidirectional waves in spacetime, then these bidirectional waves, will automatically exhibit relativistic contraction and the mechanism of relativistic contraction of even the nucleus of an atom would be conceptually understandable.

Pages 5-13 and 5-14

Compton Frequency: We will return to figures later, but first we want to calculate the rotational frequency of the rotating dipole. If we presume that a rotar is a confined wave traveling at the speed of light, it is necessary to assign a frequency to this wave. Is it possible to obtain an implied frequency from a particle's de Broglie wave characteristics? In chapter #1 we showed that confined light exhibits many properties of a particle. These include the appearance of the optical equivalent of de Broglie waves when the confined light is moving relative to an observer. If we were only able to detect the optical de Broglie waves present in a moving laser, it would be possible to calculate the frequency of the light in the moving laser. Similarly, we can

attempt to calculate a rotar's frequency from its de Broglie waves. We know a particle's de Broglie wavelength ($\lambda_d = h/mv$) and the de Broglie wave's phase velocity ($w_d = c^2/v$). From these we obtain the following angular frequency ω .

$$\begin{aligned} v_d &= \frac{w_d}{\lambda_d} = \left(\frac{c^2}{v}\right) \left(\frac{mv}{h}\right) = \frac{mc^2}{h} & v &= \text{frequency} \\ \omega &= 2\pi v_d = \frac{2\pi mc^2}{h} = \frac{mc^2}{\hbar} = \omega_c \\ \omega &= \omega_c = \frac{mc^2}{\hbar} = \frac{c}{\lambda_c} = \frac{E_i}{\hbar} = \text{Compton angular frequency} \end{aligned}$$

This calculation says that a rotar's angular frequency is equal to a rotar's Compton angular frequency ω_c . We will presume that this is a rotar's fundamental frequency of rotation. While the de Broglie wavelength and phase velocity depend on relative velocity, the velocity terms cancel in the above equation yielding a fundamental frequency (Compton frequency) that is independent of relative motion. The reasoning in this calculation can be conceptually understood by analogy to the example in chapter 1 of the bidirectional waves in the moving laser.

A rotar's Compton wavelength will be designated λ_c . The connection between a rotar's Compton wavelength and de Broglie wavelength λ_d is very simple.

$$\lambda_c = \lambda_d \gamma (v/c) \quad \text{where } \gamma \text{ is the special relativity gamma: } \gamma = [1 - (v/c)^2]^{-1/2}$$

The simplicity of these equations show the intimate relationship between a rotar's de Broglie wavelength and Compton wavelength. For another example, imagine a generic "particle" that might be a composite particle such as an atom or molecule. This "particle" is at rest in our frame of reference. Suppose that this particle emits a photon of wavelength λ_γ . This photon has momentum $p = h/\lambda_\gamma$. Therefore the emission of this photon imparts the same magnitude of momentum to the emitting particle but in the opposite vector direction (recoil). Now, the particle is moving relative to our frame of reference. What is the de Broglie wavelength of the recoiling particle in our frame of reference?

$$\begin{aligned} \lambda_d &= h/p & \text{set } p &= h/\lambda_\gamma \\ \lambda_d &= \lambda_\gamma \end{aligned}$$

Therefore, we obtain the very interesting result that the de Broglie wavelength of the recoiling particle equals the wavelength of the emitted photon. In Appendix A of chapter 1 it was proven that a confined photon with a specific energy exhibits the same inertia as a fundamental particle with the same energy. Another way of saying this is that a particle with de Broglie wavelength λ_d exhibits the same magnitude of momentum as a photon with the same wavelength. Furthermore, in chapter 1 we saw the similarity between de Broglie waves with wavelength λ_d and the propagating interference patterns with modulation wavelength λ_m . Imparting

momentum $p = h/\lambda_\gamma$ to either a fundamental particle with Compton wavelength λ_c or a confined photon with the same wavelength will produce the result: $\lambda_d = \lambda_m = \lambda_\gamma$. Therefore, it is proposed that this offers additional support to the contention that fundamental particles are composed of a confined wave in spacetime with a wavelength equal to the particle's Compton wavelength λ_c . In the remainder of this book we will often use an electron in numerous examples. An electron has the following Compton frequency, Compton angular frequency and Compton wavelength:

Electron's Compton frequency $\nu_c = 1.24 \times 10^{20}$ Hz

Electron's Compton angular frequency $\omega_c = 2\pi \nu_c = 7.76 \times 10^{20}$ s⁻¹

Electron's Compton wavelength $\lambda_c = 2.43 \times 10^{-12}$ m

Electron's reduced Compton wavelength $\lambda_c = 3.86 \times 10^{-13}$ m ($\lambda_c = c/\omega_c$)

Radius of a Rotar: Once we know the rotar's frequency of rotation, we can calculate the rotar's radius assuming speed of light motion. The circle in Figure 5-1 is an imaginary circle with a circumference one Compton wavelength. The radius of the circle one Compton wavelength in circumference is equal to the rotar's reduced Compton wavelength λ_c .

$$\lambda_c = c/\omega_c = \lambda_c/2\pi = \hbar/mc = \hbar c/E_i$$

Where:, λ_c = reduced Compton wavelength = rotar's radius; λ_c = Compton wavelength,

E_i = rotar's internal energy

In quantum mechanics, this distance λ_c is the logical division where a particle's quantum effects become dominant. For example, a fundamental particle of mass m can move discontinuously over a distance λ_c . A particle can go out of existence, or come into existence, for a time equal to λ_c/c . Essentially, the distance λ_c is a rotar's natural unit of length and $1/\omega_c$ is a rotar's natural unit of time. In chapters 6 and 8 it will be shown that the gravitational and electrostatic force exerted by a fundamental particle become much easier to understand when the distance between particles is expressed in the number of reduced Compton wavelengths rather than the number of meters.

Pages 10-11 to 10-19

Model of the External Volume: Figure 10-1 is a simplified representation of the standing dipole waves that surround a rotar. Recall that the rotar is attempting to radiate away its energy and emits dipole waves with frequency ω_c and amplitude $A_r = L_p/r$. The few rotars that are stable or semi-stable must form a resonance with the surrounding vacuum energy that eliminates the energy loss but leaves both standing waves and non-oscillating strains in spacetime as previously discussed. All the figures in this chapter deal with the standing waves associated with the oscillating part of the electric field. These standing waves have amplitude $A_e = L_p/\mathcal{N}^2$ and angular frequency ω_c . Figure 10-1 is the first in this series of figures and this figure has been greatly simplified compared to an actual rotar. The rotating dipole has been replaced by a simple monopole source of waves. In fact, we will use a monopole emitter for the first series of figures because the initial illustrations are easier to understand without the added complexity of a

rotating dipole source. The figures will later be illustrated using a dipole source when this source becomes important to the illustration.

Initially we will imagine that figure 10-1 represents sound waves being emitted by a monopole emitter of sound waves at the center circle and being reflected by a spherical reflector outside of the area shown in the figure. The interaction between the emitted and reflected waves forms the standing waves depicted in figure 10-1 and subsequent figures. An acoustic monopole emitter can be thought of as a sphere that expands and contracts its radius at an acoustic frequency.

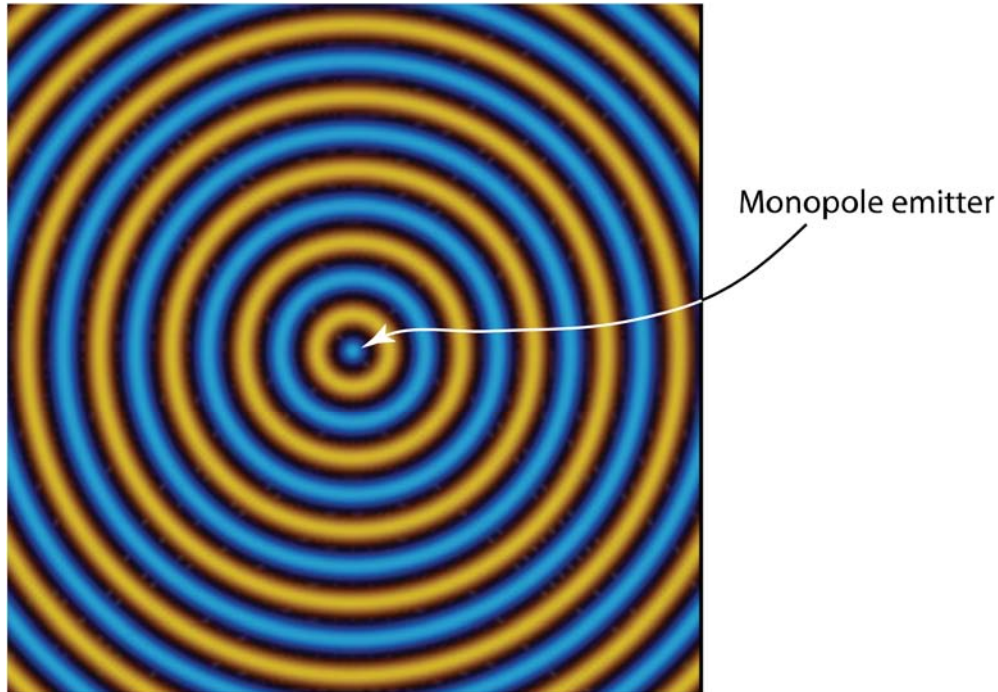


FIGURE 10-1 Monopole emission pattern

Figure 10-1 shows standing waves in an acoustic medium depicted at a moment in time. The blue regions can represent regions of maximum acoustic pressure and the yellow regions can represent regions of minimum acoustic pressure. A half cycle later the standing waves will reverse and regions that previously had maximum pressure will have minimum pressure. The black regions between the yellow and blue regions would be the wave nulls in this representation, but there is another way of depicting this standing sound wave.

The black regions have the maximum pressure gradient. This means that the black regions have the maximum kinetic energy of the acoustic medium. Therefore, there is another way of representing the standing acoustic wave where we emphasize the kinetic energy of molecules. In this type of representation the black regions would be depicted as regions of maximum kinetic

energy, not the nulls shown above. In fact the energy in the standing acoustic wave is just being transferred between energy in compression/rarefaction and kinetic energy.

We will now switch to considering figure 10-1 as representing standing waves in spacetime. The vacuum fluctuations that form spacetime have a vastly larger energy density than the energy density of a rotar. As previously discussed, the pressure of vacuum energy is stabilizing the rotar and exerting the necessary pressure to confine the energy density of the rotar. Figure 10-1 represents a moment in time where the disturbance caused by the presence of the rotar results in standing waves in the surrounding vacuum energy. These standing waves fluctuate both the rate of time and proper volume. Regions of fast time are shown in blue and regions of slow time are shown in yellow. A half cycle later the fast and slow time regions will reverse. The black regions between yellow and blue have the maximum gradient in the rate of time. These regions are equivalent to the grav field previously explained. Just like the standing sound wave, there really are no nulls in the standing wave in spacetime. The regions of fluctuating rate of time have the same energy density as the regions of maximum grav field (maximum rate of time gradient). The total wave energy is constant ($\sin^2\theta + \cos^2\theta = 1$).

Wavelets: All dipole waves in spacetime are proposed to have propagation characteristics that are similar to the Huygens Principle in optics. The Huygens principle assumes that every point on an advancing wavefront of an electromagnetic wave is the source of a new disturbance. The electromagnetic wave may be regarded as the sum of these secondary waves (called “wavelets”). Reflection, diffraction and refraction are explained by assuming that all parts of an electromagnetic wave are the source of these new wavelets. The surface that is tangent to any locus of constant phase of wavelets can be used to determine the future position of the wave.

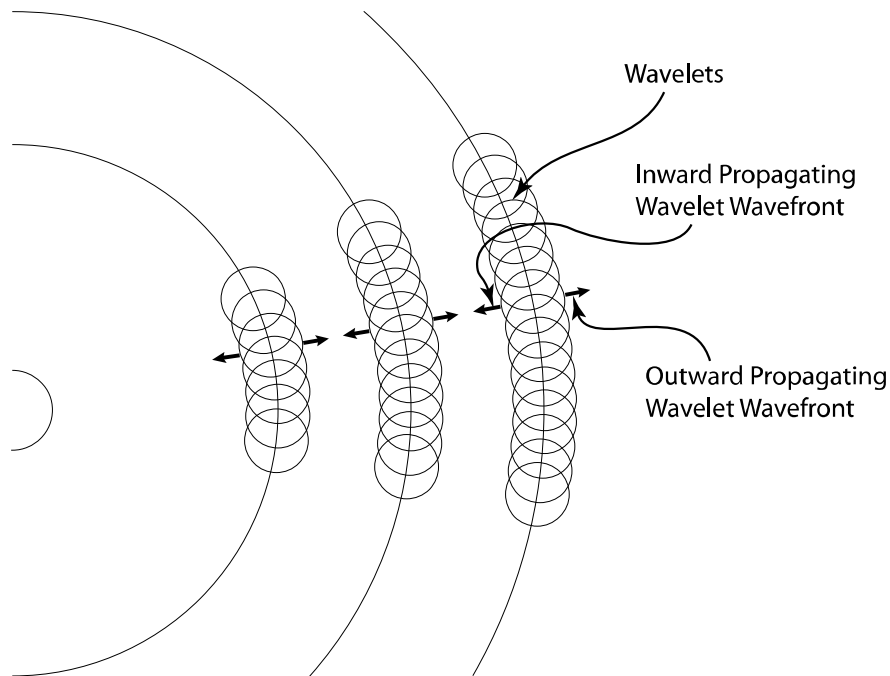


FIGURE 10-2 Simplified representation of waves propagating in spacetime. Each component becomes the source of a new wavelet.

As originally formulated by Christiaan Huygens, the Huygens Principle requires that the wavelets are hemispherical and only radiate into the forward hemispherical direction of the propagation vector. A modification of this was made by Gustav Kirchhoff where the wavelets emit into an amplitude distribution of $\cos^2(\theta/2)$. This distribution has maximum amplitude in the forward direction and zero amplitude in the reverse direction. The result is the classical Huygens-Fresnel-Kirchhoff principle that accurately describes diffraction, reflection and refraction. This will be discussed in more detail in chapter 11.

It is proposed that the few frequencies that form rotars interact with vacuum energy in a way that allows them to emit wavelets that propagate into a complete spherical pattern as shown in Figure 10-2. With this hypothesis the $\cos^2(\theta/2)$ amplitude distribution of the wavelets of light is not shared by the wavelets of vacuum energy that stabilize rotars. The conditions that stabilize rotars require that both a forward propagating wave and an equal backwards propagating wave be formed in the external volume. This is accomplished if each wavelet propagates into a spherical disturbance pattern as shown in figure 10-2. These spherical wavelets add together to produce the next generation of dipole waves in spacetime. This results in wavefronts propagating in both the forward and backward radial directions. These new wavefronts are labeled inward propagating and outward propagating. In the tangential direction there is incoherent addition that produces cancellation. If the energy flow is equal in both directions, the result is standing waves in the external volume of a rotar. Standing waves are oscillating waves

that have fixed regions of nodes and antinodes. They possess energy, but there is no continuous energy drain.

Path Integral: A key point here is that the wavelets of dipole waves in spacetime explore all possible paths between two points. Furthermore, the amplitude at any point is the coherent sum (amplitude and phase) of these waves. The intensity at any point is the square of the amplitude sum. This concept gives a physical interpretation to the path integral operation of quantum electrodynamics. It is a stretch to explain how point particles explore all possible paths between events, but waves in spacetime that form new wavelets intrinsically accomplish this task. Again, this proposed spacetime based explanation makes quantum mechanical operations conceptually understandable while the point particle model has numerous mysteries.

This explanation that involves backwards propagating waves sounds good, but there is a problem. If this was the only mechanism stabilizing a rotar, the residual standing waves would be much larger than the calculated amplitude of $A_e = \sqrt{\alpha} L_p / \mathcal{N}^2$ required for the standing wave part of the electric field. There appears to be an additional unknown mechanism generated in vacuum energy that forms a wave that provides additional cancelation. These standing waves remain even when the non-oscillating component of the electric field has been canceled. If others choose to model these standing waves, it should be noted that accurate modeling of the Huygens Principle in optics requires that the modeling must be done in three spatial dimensions¹. If the Huygens's Principle is modeled in only 2 spatial dimensions, there is incomplete cancelation of waves that do not contribute to a wavefront.

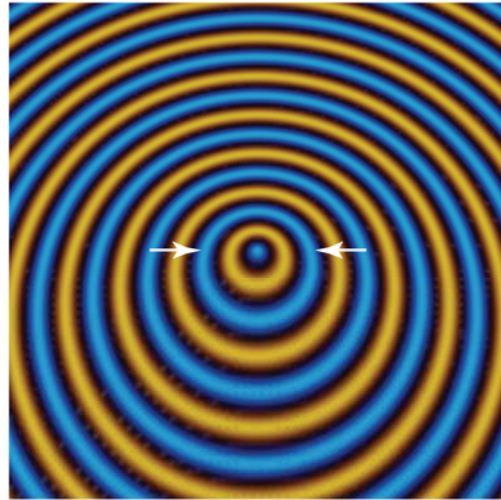
¹ <http://www.mathpages.com/home/kmath242/kmath242.htm>

Outward propagating waves



FIGURE 10-3 Doppler shift on outward propagating waves.

Inward propagating waves



↓
Direction
of Relative
Motion

FIGURE 10-4 Doppler shift on inward propagating waves.

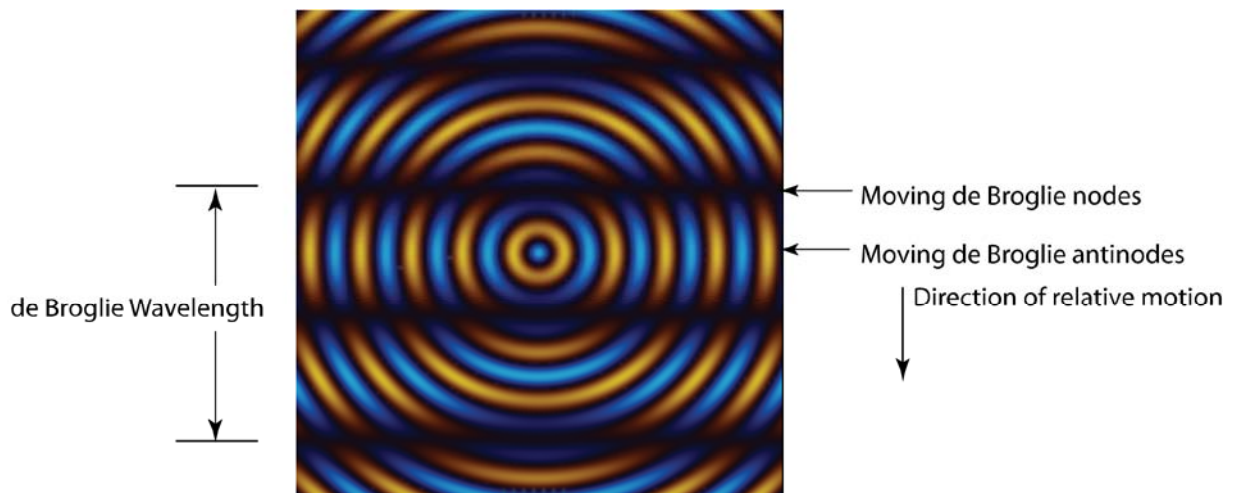


FIGURE 10-5 Linear de Broglie waves obtained from the translation of the rotar model (except monopole source)

de Broglie Waves: In chapter 1 it was shown that a laser contains light traveling in opposite directions. When the waves in this laser are observed from a stationary frame of reference, the bidirectional light forms standing waves. In other words, the standing waves are stationary relative to the laser mirrors. When the laser is translated relative to an observer, the standing light waves are still stationary relative to the moving mirrors, but the moving frame of reference means that the observer sees the light being Doppler shifted up in frequency in the direction of travel and being Doppler shifted down in frequency in the opposite direction. The superposition

of these two Doppler shifted beams of light produces what appears to be a moving envelope of waves.

Figure 1-1 shows the moving envelope of waves and moving laser mirrors. An analogy is proposed to be present when a rotar is observed in a moving frame of reference. It is desirable to examine the de Broglie waves of a rotar in greater detail. Figure 10-3 is similar to Figure 10 - 1, but there are two differences. First, Figure 10-3 shows waves propagating only away from the monopole source (arrows pointing away from the source). Second, Figure 10-3 shows the monopole source moving downward relative to the observer. The combination of these two factors produces the Doppler wave pattern shown. Figure 10-4 also has a downwards moving frame of reference, but the difference is that only waves propagating towards the source (inward propagation) are shown with arrows pointing towards the source.

The wavelets previously shown in figure 10-2 means that waves are simultaneously propagating both towards the source and away from the source. This means that a moving source will produce a wave pattern that is a superposition of figures 10-3 and 10-4. When we add these two patterns together we obtain the result shown in Figure 10-5. It is surprising to see that we obtain a linear wave pattern from the superposition of spherical waves in a moving frame of reference. These are the rotar's de Broglie waves. They have all the correct characteristics – correct de Broglie wavelength, correct de Broglie phase velocity and the correct de Broglie group velocity. Moving the rotar model produces the rotar equivalent of de Broglie waves.

This figure is not static. Not only is there translation relative to the observer, but the dark interference fringes are moving at a speed faster than the speed of light. For example, if the rotar model is moving at 1% of the speed of light relative to an observer, then the interference pattern is moving in the same direction as the relative motion, but at 100 times the speed of light ($w_d = c^2/v$). Also notice that there is a phase shift going across the dark interference pattern. This is represented by a reversal of color following a wave across the dark de Broglie null.

Figure 10-5 makes no attempt to show that the amplitude decreases with radial distance from the source. Figure 10-6 is a 3-dimensional graphical representation of Figure 10-5 with the added feature of a $1/r$ amplitude dependence. The actual amplitude should fall off proportional to $1/r^2$, but this sharp decrease in amplitude makes it difficult to see the de Broglie modulation wave.

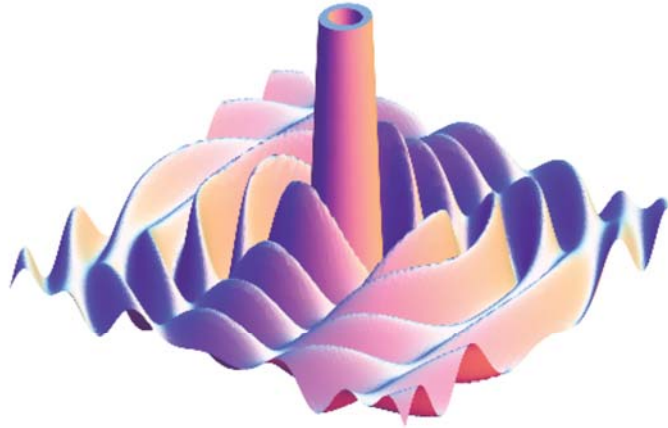


FIGURE 10-6 Three Dimensional Wave Plot Showing DeBroglie Waves and a Radial Amplitude Dependence

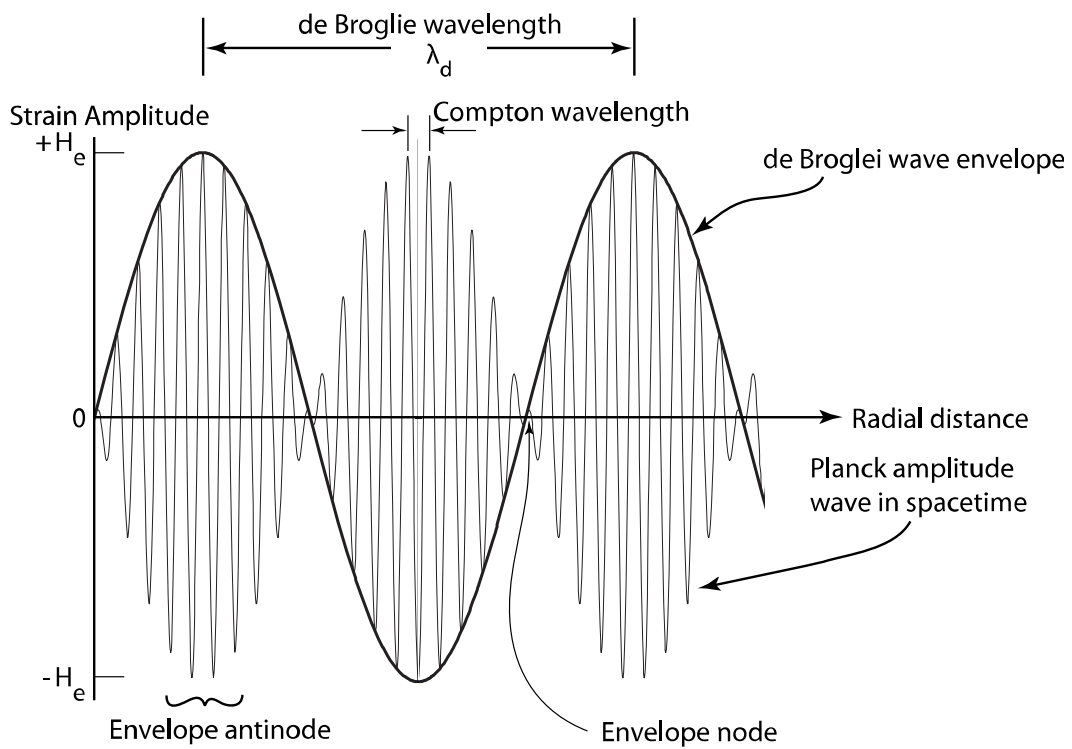


FIGURE 10-7 Graphical representation of a portion of the spacetime waves that form the external volume of a moving rotar.

Strain Amplitude Graph: It is easiest to explain the de Broglie modulation wave using Figure 10-7. This figure is a graph of the waves in figure 10-5 (radial cross-section). In figure 10-7, the high frequency waves are designated as “dipole waves in spacetime”. When a rotar is stationary relative to the observer, then all the dipole waves in spacetime have equal amplitude. At this stationary condition the frequency of these waves is the rotar’s Compton frequency ($\sim 10^{20}$ Hz for an electron) and the wavelength of these waves is the rotar’s Compton wavelength λ_c . When the rotar is moving relative to the observer, then the rotar’s de Broglie wave appears. This is just the modulation envelope that results from the different Doppler shift for waves propagating away from the rotar’s rotar volume and towards the rotar volume.

Figure 10-7 shows a graphical representation of the rotar’s de Broglie wavelength λ_d . This graph plots strain amplitude versus radial distance r . Only a short radial segment is shown. There should be a radial decrease in amplitude, but the short radial distance depicted does not show this decrease in amplitude. In the external volume of a rotar the fundamental traveling wave with amplitude L_p/r has been canceled leaving behind the standing wave responsible for the rotar’s electric charge with amplitude of $A_e = \sqrt{\alpha} A_\beta/\mathcal{N}^2$. The nonlinear effect responsible for the oscillating portion of gravity is too small to be shown. Therefore, the Y axis of this graph is the strain amplitude A_e . The maximum value of A_e is the value given by the equation $A_e = \sqrt{\alpha} A_\beta/\mathcal{N}^2 = \sqrt{\alpha} L_p\lambda_c/r^2$.

To give an idea of scale, the approximate Compton wavelength λ_c is shown. An electron’s Compton wavelength is about 2.43×10^{-12} m. The de Broglie wavelength λ_d depends on relative velocity (v) and is illustrated as being approximately 20 times longer than the Compton wavelength in this example. Therefore, the de Broglie wavelength would be approximately 5×10^{-11} m in this example. The Compton wavelength λ_c and the de Broglie wavelength λ_d are related as follows: $\lambda_c = (v/c)\lambda_d$ (approximation $v \ll c$). Therefore, this figure illustrates the de Broglie wave pattern if an electron is traveling at about 5% the speed of light ($\lambda_d \approx 20\lambda_c$ in this figure).

The Y axis of this graph is strain amplitude which can be expressed either as a spatial strain (meters/meter) or as a temporal strain (seconds/second). Both ways of expressing this give the same dimensionless number for a specific point in space and instant in time. Suppose our observation point at a particular instant is one micrometer (10^{-6} meters) from an electron that is moving past us at 5% the speed of light. We can then quantify the strain amplitude depicted in Figure 10-7. Using $A_e = \sqrt{\alpha} A_\beta/\mathcal{N}^2 = \sqrt{\alpha} L_p\lambda_c/r^2$ and substituting $r = 10^{-6}$ m and $\lambda_c = 3.86 \times 10^{-13}$ m for an electron, we obtain: $A_e = 5.3 \times 10^{-37}$. This is the maximum value of A_e above and below the zero strain line (the “x” axis).

It is possible to calculate the displacement of spacetime required to produce this amount of dimensionless strain. This strain exists over approximately one radian of the wave which is a

distance equal to λ_c . For an electron $\lambda_c = 3.86 \times 10^{-13}$ m therefore $A_e \times \lambda_c \approx 2 \times 10^{-49}$ m. Therefore, the spatial displacement of spacetime (displacement amplitude) which causes the strain amplitude illustrated here is smaller than Planck length by a factor of about 10^{14} . If we would have chosen to work in the temporal domain we would obtain the same dimensionless strain which could be thought of as seconds/second. The temporal displacement amplitude causing this strain would then be $A_e/\omega_c \approx 6.8 \times 10^{-58}$ s. This is smaller than Planck time and the difference is again a factor of about 10^{14} .